Journal of Southeast University (English Edition) Vol. 30, No. 4, pp. 411 −415 Dec. 2014 ISSN 1003—7985

Measurement of spatiotemporal characteristics of femtosecond laser pulses by a modified single-shot autocorrelation

Deng Yangbao[1,2] Deng Shuguang[2] Xiong Cuixiu[2] Zhang Guangfu[2] Tian Ye[2] Shen Lianfeng[1]

([1]National Mobile Communications Research Laboratory, Southeast University, Nanjing 210096, China)

([2]College of Communication and Electronic Engineering, Hunan City University, Yiyang 413000, China)

Abstract: To overcome the shortcomings of the single-shot autocorrelation (SSA) where only one pulse width is obtained when the SSA is applied to measure the pulse width of ultrashort laser pulses, a modified SSA for measuring the spatiotemporal characteristics of ultrashort laser pulses at different spatial positions is proposed. The spatiotemporal characteristics of femtosecond laser pulses output from the Ti: sapphire regenerative amplifier system are experimentally measured by the proposed method. It was found that the complex spatial characteristics are measured accurately. The pulse widths at different spatial positions are various, which obey the Gaussian distribution. The pulse width at the same spatial position becomes narrow with the increase in input average power when femtosecond laser pulses pass through a carbon disulfide (CS_2) nonlinear medium. The experimental results verify that the proposed method is valid for measuring the spatiotemporal characteristics of ultrashort laser pulses at different spatial positions.

Key words: spatiotemporal characteristics; modified single-shot autocorrelation; femtosecond laser pulses; ultrafast laser technology

doi: 10.3969/j. issn. 1003 −7985. 2014. 04. 002

With the rapid development of the ultrafast laser technology, the pulse width of ultrashort laser pulses has entered the attosecond field[1−2]. Ultrafast laser technology has broad application prospects in many fields, such as optical communication, laser-plasma interaction, and pump-probe spectroscopy[3−5]. The ultrashort laser pulse is used as a very short time probe, which provides an important tool for investigation in the microscopic world. Before ultrashort laser pulses are used for practical applications, it is necessary to properly characterize their main parameters, including energy, power, spectrum, spatial beam, temporal shape, pulse width and phase. It is easy to measure the energy, power, spectrum and spatial shape directly, but it is more difficult to measure the temporal shape, pulse width and phase directly due to the limitations of the instruments.

There are two types of methods for measuring the temporal shape and pulse width. One is a direct electronic technique, consisting of fast photodiodes and high-bandwidth oscilloscopes[6], which are limited to the several picoseconds. Therefore, fast photodiodes and high-bandwidth oscilloscopes are not suitable for recording the temporal profile of an ultrashort (femtosecond or attosecond) laser pulse. The only detector that reaches a time resolution below one picosecond is the streak camera[7], which is also not suitable for measuring the temporal profile of the ultrashort laser pulse. The other is the optical correlation technique, mainly including intensity autocorrelation[8−10], intensity cross-correlation[11−12], frequency resolved optical gating (FROG)[13−14] and spectral phase interferometry for direct electric-field reconstruction (SPIDER)[15−16]. The intensity autocorrelation technique uses a model to retrieve the pulse shape according to the experimental data. The intensity cross-correlation technique characterizes the temporal shape of a complex pulse directly by measuring the sum-frequency signal light, whose resolution primarily depends on the pulse width of a probe pulse[11]. Unfortunately, the autocorrelation and cross-correlation only measure the pulse shape and pulse width, and do not measure the phase characteristics. FROG retrieves the electric field of ultrashort laser pulses based on a complex iterative algorithm. SPIDER does not give the pulse width information directly, but reconstructs the pulse shape and pulse width by the Fourier transform. FROG and SPIDER are very useful for measuring the amplitude and phase of the ultrashort laser pulse, but they are more complex in experiment operations.

In all the above methods, the SSA's operation is simple and convenient, and it is also suitable for measuring the ultrashort laser pulse with a pulse width of hundreds of femtoseconds. However, only one pulse width of the whole beam is obtained when the SSA is used to measure the pulse width of ultrashort laser pulses. In fact, pulse stretching and compression are asymmetric, causing the pulse widths at different spatial positions to be different due to the effect of the residual spatial chirp. For the

Received 2014-05-07.

Biographies: Deng Yangbao (1983—), male, doctor, lecturer; Shen Lianfeng (corresponding author), male, professor, lfshen@seu.edu.cn.

Foundation items: The National Natural Science Foundation of China (No. 61171081, No. 61471164), the Natural Science Foundation of Hunan Province (No. 14JJ6043).

Citation: Deng Yangbao, Deng Shuguang, Xiong Cuixiu, et al. Measurement of spatiotemporal characteristics of femtosecond laser pulses by a modified single-shot autocorrelation[J]. Journal of Southeast University (English Edition), 2014, 30(4): 411 −415. [doi: 10.3969/j. issn. 1003 −7985. 2014. 04. 002]

shortcomings of the SSA and the aforementioned reasons, a modified SSA is proposed for measuring the spatiotemporal characteristics of the femtosecond laser pulse. The proposed method not only measures the spatiotemporal characteristics of a laser pulse at different spatial positions, but also characterizes the temporal evolution of a pulse at the same spatial position after nonlinear propagation.

1 Measurement Principle Analysis

SSA is used to measure the pulse width of ultrashort laser pulses, which mainly measures the cross distribution of the second harmonic (SH) beam. If the pulse has the Gaussian time shape, the cross size D of the SH beam depending on the pulse width T of base frequency laser pulse is written as[7]

$$T = \frac{\Delta t D}{\sqrt{2} Z_0} \tag{1}$$

where Δt is time delay, and Z_0 is the center of the SH beam cross distribution. It should be noted that Eq. (1) is correct under the condition of

$$nuT \ll d \tan\left(\frac{\Psi}{2}\right) \tag{2}$$

where n is the refraction index of the nonlinear crystal; u is the light velocity of the base frequency laser pulse in the crystal; T is the pulse width of base frequency laser pulse at FWHM; d is the beam diameter of the base frequency beam at the FWHM of intensity; Ψ is the angle between the two beams outside the crystal.

It is clear that direct measurement of Δt and Z_0 is rather difficult. With the help of optical delay line, it is possible to change the value of Δt. Simultaneously, the center Z_0 of the SH beam is changed. If two centers Z_{01} and Z_{02} are corresponding to the micrometric head positions L_1 and L_2, the time delay differential can be written as

$$\Delta t_1 - \Delta t_2 = \frac{2(L_1 - L_2)}{c} \tag{3}$$

where c is the light velocity of the base frequency beam in vacuum. On the other hand, the time delay differential can be obtained from Eq. (1),

$$\Delta t_1 - \Delta t_2 = \frac{\sqrt{2} T (Z_{01} - Z_{02})}{D} \tag{4}$$

By Eqs. (3) and (4), we can obtain

$$\frac{2(L_1 - L_2)}{c} = \frac{\sqrt{2} T (Z_{01} - Z_{02})}{D} \tag{5}$$

By Eq. (5), the pulse width T can be written as

$$T = \frac{\sqrt{2} D \ (L_1 - L_2)}{(Z_{01} - Z_{02}) c} \tag{6}$$

which is the basic expression for measuring the pulse width based on the SSA.

The experimental setup of the SSA and the transverse spatial intensities distributions of the SH beam are shown in Fig. 1. In Fig. 1(a), M1-M5 are silver-coated plane mirrors; BS is the beam splitter; DL represents delay line; BBO is β-barium borate crystal; and A represents the adjustable neutral density attenuator. Using the experimental setup of Fig. 1(a), the initial pulse width of chirp-free femtosecond laser pulse is measured. The measured transverse spatial intensities distributions of the SH beam are shown in Fig. 1(b). From Fig. 1(b), the parameters are obtained as follows: $Z_{01} - Z_{02} = 0.315$ mm, the cross size D of the SH beam at Z_{01} and Z_{02} are identical, $D = 0.225$ mm, $L_1 - L_2 = 0.03$ mm, $c = 3 \times 10^{-4}$ mm/fs. According to Eq. (6), the pulse width T is about 100 fs. The pulse width will be broadened when the femtosecond laser pulse is added to an initial chirp. The pulse width is also measured based on the experiment setup of Fig. 1(a). In the process of measuring, if the delay line is invariable ($L_1 - L_2 = 0.03$ mm), $Z_{01} - Z_{02}$ is also invariable ($Z_{01} - Z_{02} = 0.315$ mm). It was found that the pulse width T varies with the cross size D of the SH beam according to Eq. (6). For example, in the initial condition of $D_1 = 0.225$ mm, the pulse width $T_1 = 100$ fs; if D is increased ($D_2 = 0.365$ mm), the pulse width is estimated $T_2 =$

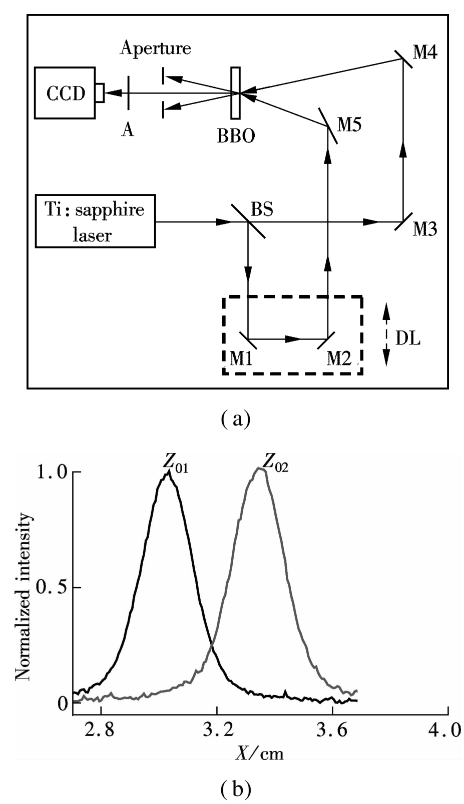

Fig. 1 Experimental setup of SSA and transverse spatial intensity distributions of the SH beam. (a) Schematic diagram of SSA; (b) Transverse spatial intensity distributions of the SH beam at delay L_1 and L_2

$\left(\frac{D_2}{D_1}\right)T_1 = \left(\frac{0.365}{0.225}\right) \times 100$ fs $= 162$ fs. Therefore, the pulse width of the base frequency laser pulse is estimated by measuring the cross size D of the SH beam directly. In other words, the cross size D of the SH beam characterizes the variation of the pulse width of the base frequency laser pulse directly. During the SSA measurement, a collimated laser pulse is separated into two laser pulses by the beam splitter, then only one SH beam is obtained after the BBO crystal due to the identical spatial shape of the two laser pulses. So only one cross size D of the SH beam is measured, which shows that only one pulse width of the whole base frequency laser pulse is obtained. If the experimental setup of the SSA is modified, a collimated laser pulse is separated into two laser pulses by the beam splitter, where one is used as the pump laser pulse and the other is used as the probe laser pulse controlled by a device. The spatial shape of the pump laser pulse is invariant, but the spatial shape of the probe laser pulse is variant. Different cross sizes of the SH beam are obtained when the probe laser pulse probes different spatial positions of the pump laser pulse (base frequency laser pulse). Therefore, the pulse widths of the base frequency laser pulse at different spatial positions are measured indirectly due to the differing cross sizes of the SH beam. At the same time, the measured SH beam characterizes the spatial distribution characteristics of the base frequency laser pulse at different spatial positions directly.

2 Experimental Setup of Modified SSA

The experimental setup of the modified SSA and spatial intensities distributions of the probe laser pulse after a slit are shown in Fig. 2. In Fig. 2(a), A1 and A2 represent the adjustable neutral density attenuators and SM is the spatial modulation. The femtosecond laser pulse is output from the Ti: sapphire regenerative amplifier system (Coherent Libra S), whose main parameters are as follows: the pulse width is 100 fs; central wavelength is 800 nm and then repetition frequency is 1 kHz. A collimated laser pulse is separated into two laser pulses by a beam splitter, where one is used as a pump laser pulse and the other is used as a probe laser pulse that is controlled by a slit. The reflectivity of the beam splitter is about 20%. The sum-frequency light with the 400 nm wavelength is generated in the BBO crystal (7 mm × 7 mm × 0.7 mm) by a small angle nonlinear sum-frequency interaction between the pump laser pulse and the probe laser pulse. The charge-coupled device CCD (Coherent Laser Cam-HRTM, 1 280 × 1 024 pixel, resolution: 6.7 μm × 6.7 μm) has two functions. One is used to measure the spatial characteristics of the pump laser pulse directly, and the other is used to measure the pulse width evolution of the pump laser pulse at different spatial positions indirectly based on the principle in Section 1. As the probe laser pulse is controlled by a silt, the transverse spatial profile of the probe laser pulse after passing through a slit is approximately a sinc function distribution[17], as shown in Fig. 2(b). The main peak becomes narrow and the side-lobes are very weak with the increment of the slit width. However, the intensities of the side-lobes increase gradually when the slit width is wider than 0.67 mm. In order to achieve the narrowest spatial distributions of the main peak and ensure that the side-lobes have little effect on the measurement results, the slit width is adjusted to 0.67 mm (see Fig. 2(b)).

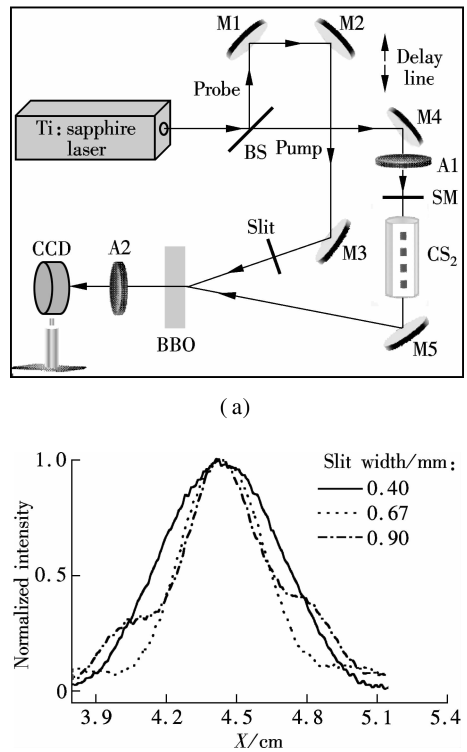

(a)

(b)

Fig. 2 Experimental setup of modified SSA and spatial intensities distributions of probe laser pulse. (a) Schematic diagram of modified SSA; (b) Variation of the spatial intensities distributions of probe laser pulse with slit widths

3 Experimental Results and Discussion

3.1 Measurement of the spatial characteristics

The spatial intensity distribution of the pump laser pulse with a cross-silk modulation and the measured spatial characteristics of the pump laser pulse are shown in Fig. 3. In order to measure the complex transverse spatial characteristics of the pump laser pulse, the slit is vertically placed. The experimental measured transverse spatial distributions of the modulation peaks of the pump laser pulse are shown in Fig. 3(b), which is almost the same as that in Fig. 3(a). The BBO crystal is not sufficiently large for our experiment and the edge spatial intensity of the pump laser pulse is very weak, so Fig. 3(b) does not characterize the edge spatial characteristics of the pump laser pulse. The longitudinal spatial intensity distributions of the pump laser pulse with a cross-silk modulation are also measured when the slit is horizontally placed. Therefore, all the spatial intensity distributions of the ultrashort laser pulse are measured accurately based on the modified SSA.

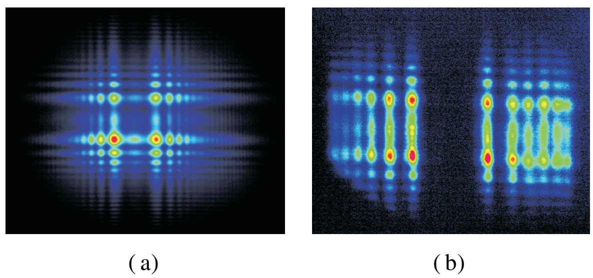

Fig. 3 Experimental results of spatial measurement. (a) Spatial intensity distribution of the pump laser pulse with a cross-silk modulation; (b) Measured transverse spatial intensity distribution of pump laser pulse

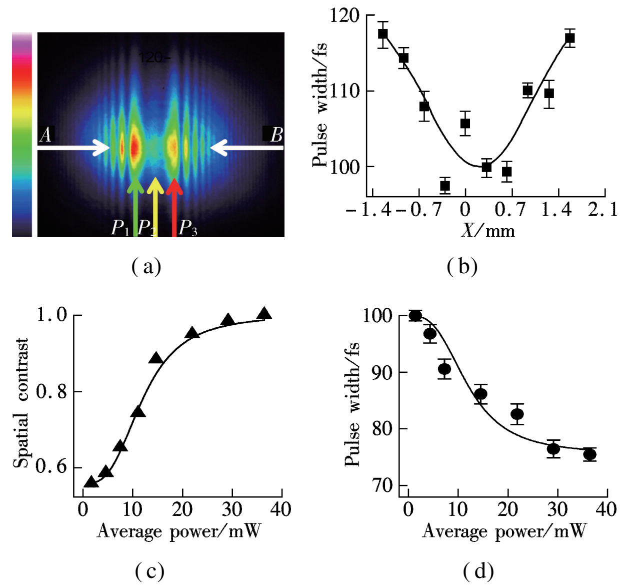

Fig. 4 Experimental results of temporal measurement. (a) Spatial intensity distribution of the pump laser pulse with a single silk modulation; (b) The measured pulse widths of pump laser pulse at different spatial positions between points A and B; (c) Variation of spatial contrast with input average power; (d) Variation of the measured temporal evolutions of pump laser pulse at P_3 position with input average power

3.2 Measurement of the temporal characteristics

The experimental measured temporal characteristics are shown in Fig. 4. As the initial spatial modulation shape of the pump laser pulse has little effect on the validity of the pulse width measurement, for convenience of spatial orientation, the pump laser pulse is added to a single silk modulation during measurement, whose spatial intensity distribution is shown in Fig. 4(a). When the slit is vertically placed, the pulse widths at different transverse spatial positions between points A and B are measured as shown in Fig. 4(b), where the solid square boxes are the experimental results and the solid curve is the Gaussian fitting results. The pulse widths at different transverse spatial positions obey the Gaussian distribution. The pulse width of the pump laser pulse at the strongest spatial modulation position P_1 is measured and then the probe laser pulse is moved in the transverse spatial direction step by step. So the pulse width at different transverse spatial positions between points A and B are measured. The pulse widths at transverse spatial positions are represented by P_1, P_2 and P_3 (see Fig. 4(a)) are 95, 106 and 100 fs (see Fig. 4(b)), respectively. The pulse width at P_3 position is the same as that measured by the SSA. Pulse broadening and compression are asymmetric, which causes the best compression in the central positions, thus the pulse widths at edge positions are wider than those of central positions due to the effect of the residual spatial chirp (see Fig. 4(b)). The pulse widths at different longitudinal spatial positions are also measured when the slit is horizontally placed. Therefore, the pulse widths of the ultrashort laser pulse at all spatial positions are measured based on the modified SSA.

Furthermore, the temporal evolution of the pump laser pulse at P_3 position after propagating in the CS_2 nonlinear medium is measured. The variation of the measured spatial contrast with input average power is shown in Fig. 4(c), where the solid triangles are the experimental results and the solid curve is the nonlinear fitting results. It is clearly seen that the spatial contrast is increased with the increment of rising power, so the pump laser pulse generates a small-scale self-focusing effect (see Fig. 4(c)). The small-scale self-focusing effect enhances the spatial intensity at P_3 position, which in turn affects the temporal evolution at this position. The measured evolution of pulse width at P_3 position is represented in Fig. 4(d), where the solid circle boxes are the experimental results and the solid curve is the nonlinear fitting results. The pulse width becomes narrower with the increase in the input average power due to the spatiotemporal coupling effect[18].

4 Conclusion

In this paper, a modified SSA is proposed for measuring the spatiotemporal characteristics of a femtosecond laser pulse at different spatial positions. After theoretical analyses on the measurement principle, the spatiotemporal characteristics of femtosecond laser pulses output from the Ti: sapphire regenerative amplifier system are measured by the proposed method. The experimental results show that the complex spatial characteristics are measured accurately when the femtosecond laser is added to a diffraction modulation. The initial pulse widths of the whole beam at different spatial positions are different due to the effect of the residual spatial chirp, which obey the Gaussian distribution. When the femtosecond laser pulse propagates in the CS_2 nonlinear medium, the pulse width at the same spatial position becomes narrow with the increase in the input average power due to the spatiotemporal coupling effect. Therefore, the experimental results verify that the proposed method is valid for measuring the spatiotemporal characteristics of ultrashort laser pulses at different spatial positions.

References

[1] Ferrari F, Calegari F, Lucchini M, et al. High-energy isolated attosecond pulses generated by above-saturation few-cycle fields[J]. *Nature Photonics*, 2010, **4**(12): 875 − 879.

[2] Baker S, Walmsley I A, Tisch J W G, et al. Femtosecond to attosecond light pulses from a molecular modulator [J]. *Nature Photonics*, 2011, **5**(11): 664 − 671.

[3] Sun X L, Skillman D R, Hoffman E D, et al. Free space laser communication experiments from Earth to the Lunar Reconnaissance orbiter in lunar orbit[J]. *Optics Express*, 2013, **21**(2): 1865 − 1871.

[4] Cairns R A, Bingham R, Norreys P, et al. Laminar shocks in high power laser plasma interactions[J]. *Physics of Plasmas*, 2014, **21**(2): 022112.

[5] Shang J Z, Ma L, Li J W, et al. Femtosecond pump-probe spectroscopy of graphene oxide in water[J]. *Journal of Physics D: Applied Physics*, 2014, **47**(9): 094008.

[6] Träger F. *Handbook of lasers and optics*[M]. Berlin: Springer, 2007: 962 − 978.

[7] Tsuchiya Y. Advances in streak camera instrumentation for the study of biological and physical processes[J]. *IEEE Journal of Quantum Electronics*, 1984, **20**(12): 1516 − 1528.

[8] Kolliopoulos G, Tzallas P, Bergues B, et al. Single-shot autocorrelator for extreme-ultraviolet radiation[J]. *Journal of Optical Society of America B*, 2014, **31**(5): 926 − 938.

[9] Moshammer R, Pfeifer T, Rudenko A, et al. Second-order autocorrelation of XUV FEL pulses via time resolved two-photon single ionization of He[J]. *Optics Express*, 2011, **19**(22): 21698 − 21706.

[10] Wei Y Z, Howard S, Straub A, et al. High sensitivity third-order autocorrelation measurement by intensity modulation and third harmonic detection[J]. *Optics Letters*, 2011, **36**(12): 2372 − 2374.

[11] Deng Y B, Yang H, Tang M, et al. Experimental research on measuring the fine structure of long pulse in time domain by synchronized ultrashort pulse[J]. *Optics Communications*, 2011, **284**(3): 847 − 851.

[12] Ma J, Yuan P, Wang Y Z, et al. Single-shot cross-correlator using a long-wavelength sampling pulse[J]. *Optics Letters*, 2011, **36**(6): 978 − 980.

[13] Wilcox D E, Fuller D F, Ogilvie J P. Fast second-harmonic generation frequency-resolved optical gating using only a pulse shaper[J]. *Optics Letters*, 2013, **38**(16): 2980 − 2983.

[14] Calò C, Schmeckebier H, Merghem K, et al. Frequency resolved optical gating characterization of sub-ps pulses from single-section InAs/InP quantum dash based mode-locked lasers[J]. *Optics Express*, 2014, **22**(2): 1742 − 1748.

[15] Pasquazi A, Peccianti M, Azaña J, et al. FLEA: Fresnel-limited extraction algorithm applied to spectral phase interferometry for direct field reconstruction (SPIDER) [J]. *Optics Express*, 2013, **21**(5): 5743 − 5758.

[16] Tsermaa B, Yang B K, Kim J S, et al. Crystal-dithering method applied to spectral phase interferometry for direct electric-field reconstruction (SPIDER) for sensitivity enhancement of the pulse phase measurement[J]. *Optics Communications*, 2011, **284**(7): 1955 − 1958.

[17] Goodman J W. *Introduction to Fourier optics*[M]. 3rd ed. Englewood: Roberts & Company, 2005: 28 − 55.

[18] Deng Y B, Fu X Q, Tan C, et al. Experimental investigation of spatiotemporal evolution of femtosecond laser pulses during small-scale self-focusing[J]. *Applied Physics B*, 2014, **114**(3): 449 − 454.

基于改进的单次自相关测量飞秒激光脉冲的时空特性

邓杨保[1,2]　邓曙光[2]　熊翠秀[2]　张光富[2]　田　野[2]　沈连丰[1]

([1] 东南大学移动通信国家重点实验室，南京 210096)
([2] 湖南城市学院通信与电子工程学院，益阳 413000)

摘要：针对单次自相关方法只能测量一个脉宽的缺点，提出一种改进的单次相关方法测量超短激光脉冲全空域中不同空间位置的时空特性. 通过实验测量了钛宝石激光器输出飞秒激光脉冲的时空特性，结果表明飞秒激光脉冲全空域中不同位置的复杂空间特性得以精密测量；不同空间位置的时间脉宽不同，它们服从高斯分布；当飞秒激光脉冲经过二硫化碳非线性介质传输后，随着输入平均功率的增加，同一空间位置的时间脉宽呈现慢慢变窄的趋势. 实验结果验证了所提方法可以有效地测量超短激光脉冲全空域中不同空间位置的时空特性.

关键词：时空特性；改进的单次自相关；飞秒激光脉冲；超快激光技术

中图分类号：TN2